Neuron
Article

Bidirectional Modulation of Incubation of Cocaine Craving by Silent Synapse-Based Remodeling of Prefrontal Cortex to Accumbens Projections

Yao-Ying Ma,[1] Brian R. Lee,[3] Xiusong Wang,[2] Changyong Guo,[1] Lei Liu,[4] Ranji Cui,[4] Yan Lan,[1] Judith J. Balcita-Pedicino,[1] Marina E. Wolf,[5] Susan R. Sesack,[1,2] Yavin Shaham,[6] Oliver M. Schlüter,[7] Yanhua H. Huang,[2,*] and Yan Dong[1,2,*]
[1]Department of Neuroscience
[2]Department of Psychiatry
University of Pittsburgh, Pittsburgh, PA 15260, USA
[3]Allen Institute for Brain Science, Seattle, WA 98103, USA
[4]School of Life Science, Northeastern Normal University, Jilin, China
[5]Department of Neuroscience, Rosalind Franklin University of Medicine and Science, North Chicago, IL 60064, USA
[6]Behavioral Neuroscience Branch, Intramural Research Program, NIDA, NIH, Baltimore, MD 21224, USA
[7]Molecular Neurobiology and Cluster of Excellence "Nanoscale Microscopy and Molecular Physiology of the Brain," European Neuroscience Institute, 37077 Göttingen, Germany
*Correspondence: huangy3@upmc.edu (Y.H.H.), yandong@pitt.edu (Y.D.)
http://dx.doi.org/10.1016/j.neuron.2014.08.023

SUMMARY

Glutamatergic projections from the medial prefrontal cortex (mPFC) to nucleus accumbens (NAc) contribute to cocaine relapse. Here we show that silent synapse-based remodeling of the two major mPFC-to-NAc projections differentially regulated the progressive increase in cue-induced cocaine seeking after withdrawal (incubation of cocaine craving). Specifically, cocaine self-administration in rats generated AMPA receptor-silent glutamatergic synapses within both infralimbic (IL) and prelimbic mPFC (PrL) to NAc projections, measured after 1 day of withdrawal. After 45 days of withdrawal, IL-to-NAc silent synapses became unsilenced/matured by recruiting calcium-permeable (CP) AMPARs, whereas PrL-to-NAc silent synapses matured by recruiting non-CP-AMPARs, resulting in differential remodeling of these projections. Optogenetic reversal of silent synapse-based remodeling of IL-to-NAc and PrL-to-NAc projections potentiated and inhibited, respectively, incubation of cocaine craving on withdrawal day 45. Thus, pro- and antirelapse circuitry remodeling is induced in parallel after cocaine self-administration. These results may provide substrates for utilizing endogenous antirelapse mechanisms to reduce cocaine relapse.

INTRODUCTION

Drug-induced alterations in glutamatergic synaptic transmission to the nucleus accumbens (NAc) have been critically implicated in drug relapse and conditioned drug effects (Kalivas, 2004; Pickens et al., 2011; Wolf and Ferrario, 2010). One recently discovered alteration is cocaine-induced generation of silent glutamatergic synapses (Brown et al., 2011; Huang et al., 2009; Koya et al., 2012; Lee et al., 2013). Silent synapses are thought to be immature glutamatergic synapses containing stable NMDA receptors (NMDARs), while AMPA receptors (AMPARs) are either absent or highly labile (Groc et al., 2006; Hanse et al., 2013; Kerchner and Nicoll, 2008). De novo generation of silent synapses may create new synaptic contacts, and subsequent unsilencing/maturation of these silent synapses by recruiting new AMPARs remodels the affected neurocircuits, not only strengthening circuitry transmission but also creating new forms of information flow to redefine future behaviors (Dong and Nestler, 2014; Hanse et al., 2013; Lee and Dong, 2011).

We recently demonstrated that silent synapse-based remodeling of basolateral amygdala (BLA) to nucleus accumbens shell (NAcSh) projections critically contributes to the development of "incubation of cocaine craving" (Lee et al., 2013), the progressive increase in cue-induced cocaine seeking after withdrawal from the drug (Grimm et al., 2001; Neisewander et al., 2000). At present, it is unknown whether other glutamatergic inputs to the NAc also undergo silent synapse-based remodeling and whether such potential circuitry remodeling plays a role in cocaine craving and relapse.

The medial prefrontal cortex (mPFC) provides a major glutamatergic input to the NAc, with the infralimbic mPFC (IL) preferentially projecting to NAcSh and the prelimbic mPFC (PrL) to the NAc core (NAcCo) (Krettek and Price, 1977; Sesack et al., 1989). There is evidence that drug priming-, cue-, and stress-induced reinstatement after extinction of cocaine-reinforced responding are critically dependent on activation of the PrL-to-NAcCo glutamatergic projections (Kalivas, 2009; Kalivas and McFarland, 2003). On the other hand, inactivation of IL-to-NAcSh glutamatergic projections reinstates cocaine seeking after extinction of the drug-reinforced responding, suggesting opposite modulation by PrL-to-NAcCo and IL-to-NAcSh projections of cocaine seeking after extinction (LaLumiere et al., 2012; Peters et al., 2008).

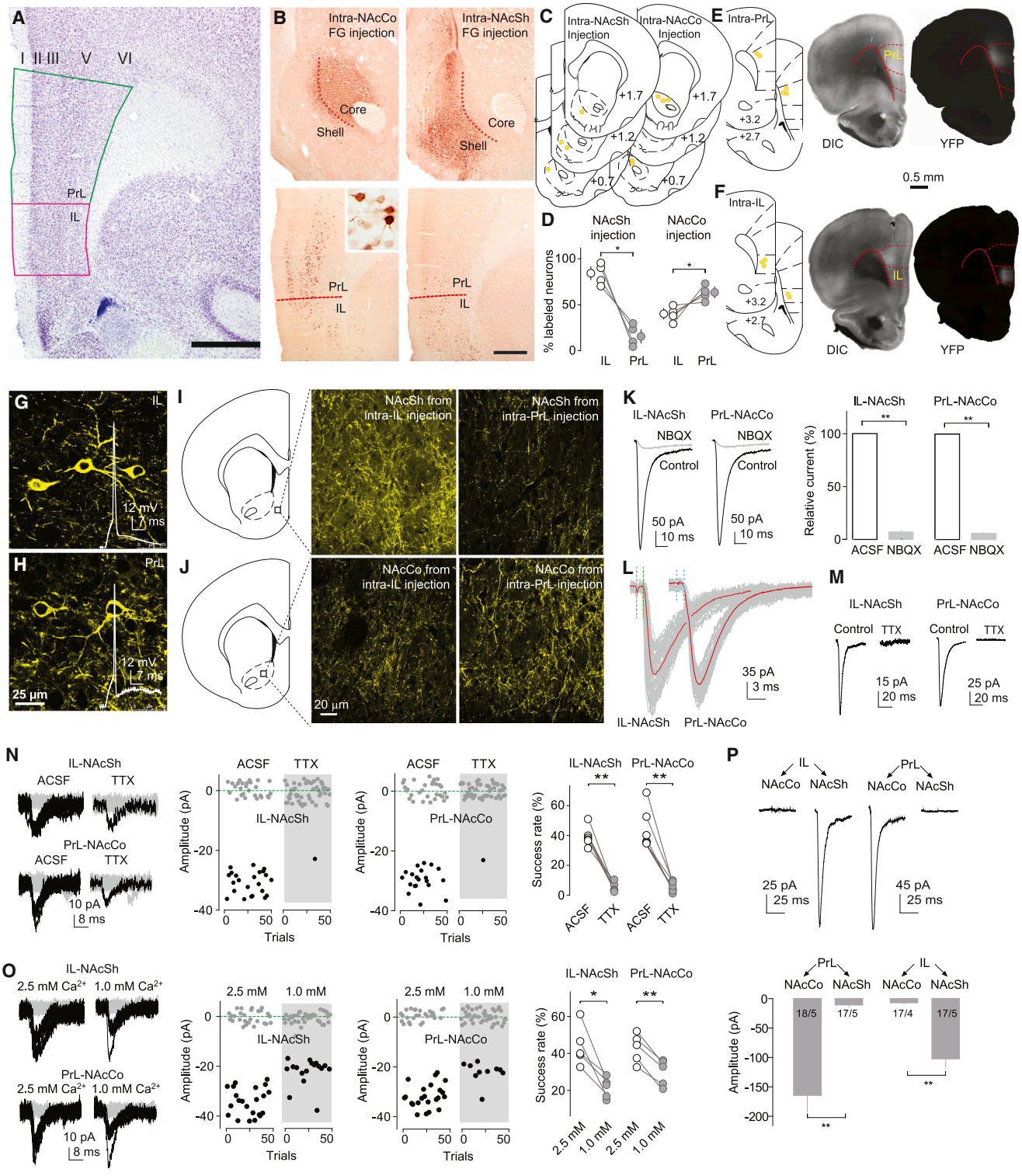

Figure 1. Anatomical and Electrophysiological Differentiation of the IL-to-NAcSh and PrL-to-NAcCo Projections in Rats

(A) A coronal section stained for Nissl showing the cytoarchitectonic boundaries of the IL and PrL in the rat, including the relatively indistinct lamina in the IL (but not the PrL) and the sudden change from a compacted to a scattered layer II at the PrL-IL border. Scale bar, 1 mm.

(B) Representative images showing immunoperoxidase labeling for FG at the injection sites involving mainly the NAcCo or NAcSh and the corresponding distribution of retrogradely labeled cells in the PrL and IL. Inset shows FG-labeled neurons at 40× magnification. Scale bar, 500 μm; 50 μm for insert.

(C) Diagrams of coronal slices showing the injection sites (yellow dots) of FG in the NAcCo of five rats (left) and ventral-medial NAcSh of four rats (right).

(legend continued on next page)

Here, we report that, similar to BLA-to-NAcSh projection (Lee et al., 2013), cocaine self-administration generated silent synapses within both the IL-to-NAcSh and PrL-to-NAcCo projections, and subsequent unsilencing/maturation of these silent synapses after withdrawal from the drug differentially remodeled the two projections via a process that involved synaptic insertion of calcium-permeable (CP) AMPARs in the IL-to-NAcSh projection and synaptic insertion of non-CP-AMPARs in the PrL-to-NAcCo projection. Most importantly, optogenetic reversal of silent synapse-based remodeling of the IL-to-NAc projection enhanced the expression of incubation of cocaine craving on withdrawal day 45, whereas reversal of the remodeling within the PrL-to-NAc projection inhibited this incubation. These results suggest that although similar silent synapse-based remodeling occurs in different glutamatergic inputs to the NAc, the behavioral consequences are projection specific. Furthermore, our results suggest that antirelapse neuroadaptations are endogenously induced in parallel with prorelapse processes.

RESULTS

Dissection of the IL-to-NAcSh and PrL-to-NAcCo Projections

Early studies suggest that the IL and PrL are anatomically differentiable in rats (Krettek and Price, 1977; Reep, 1984), with the IL preferentially projecting to the NAcSh and the PrL preferentially innervating the NAcCo (Brog et al., 1993; Sesack et al., 1989). The differentiating anatomical features established in these studies, such as the relatively clear layer separation in the PrL, but not in the IL (Krettek and Price, 1977), were observed in our studies (Figure 1A) and used as the criteria to separate these two mPFC subregions. To verify the differential projections from the IL and PrL to the NAc, we stereotaxically injected the retrograde tracer Fluoro-Gold (FG; 2%) into either the NAcSh or NAcCo of anesthetized rats and killed them 5–7 days later. In coronal slices from rats injected with FG into the NAcSh, we observed substantially more neurons labeled in IL than PrL, whereas in rats with intra-NAcCo FG injection, more FG-positive neurons were observed in PrL than IL (Figures 1B–1D), verifying the differential projections of the IL and PrL to the two NAc subregions (Brog et al., 1993).

To establish an optogenetic approach for functional examination of these two mPFC projections, we stereotaxically injected adeno-associated virus 2 (AAV2) expressing YFP-tagged channelrhodopsin 2 (ChR2) into the IL or PrL of anaesthetized rats. Three to four weeks later, we observed in coronal slices that expression of ChR2 was confined within the IL or PrL as intended (Figures 1E and 1F). After screening several optogenetic parameters, we found that laser stimulations with pulse duration of $\leq$1 ms generated reliable TTX-sensitive action potentials in ChR2-expressing IL or PrL neurons (Figures 1G, 1H, and S1A–S1D, available online). In the same rats with IL or PrL expression of ChR2, extensive fluorescent fibers that expressed ChR2 were observed in the NAcSh or NAcCo (Figures 1I and 1J), presumably originating from ChR2-expressing IL or PrL neurons, respectively.

To selectively examine synaptic transmission within the two mPFC projections to the NAc, we recorded synaptic responses induced by optogenetic stimulation (with laser pulse duration of 1 ms) from NAcSh or NAcCo medium spiny neurons (MSNs) in slices from rats injected with ChR2 into the IL or PrL. These responses, recorded at −70 mV ($V_{Reversal}[Cl^-]$ = ~−48 mV) in bath containing no GABA receptor antagonists, were inhibited by perfusion of the AMPAR-selective antagonist NBQX (5 μM), indicating that they are glutamatergic (Figure 1K). These optogenetically elicited synaptic responses exhibited a short delay after presynaptic stimulation (IL-to-NAcSh, 0.60 ± 0.16 ms, n = 19; PrL-to-NAcCo, 0.70 ± 0.13 ms, n = 20; Figure 1L), suggesting monosynaptic transmission. Thus, the 1 ms optogenetic stimulation allowed us to examine monosynaptic EPSCs at IL-to-NAcSh and PrL-to-NAcCo synapses.

To determine whether the optogenetic stimulation-induced synaptic transmission described above was action potential dependent, as occurs endogenously, we examined electrophysiological and biophysical properties of these optogenetically

(D) Summarized results showing that intra-NAcSh injections of FG resulted in a higher percentage of labeled neurons in IL (83.1% ± 5.9%) than PrL (16.9% ± 5.9%; t_3 = 5.65, p = 0.01), and that intra-NAcCo injection of FG resulted in a higher percentage of neurons labeled in PrL (61.7% ± 3.2%) than IL (38.3% ± 3.2%; t_4 = 3.60, p = 0.02).

(E) Diagrams of coronal slices showing the injection sites (yellow dots) where ChR2-expressing AAV2 was injected in the PrL of five anesthetized rats (left), and light (DIC, middle) and fluorescent (YFP, right) images showing the expression site of ChR2 3 weeks after intra-PrL injection of ChR2-AAV2.

(F) Same experimental setup as shown in (E) for intra-IL injection of ChR2.

(G and H) Confocal images showing ChR2-expressing IL (G) or PrL (H) neurons from rats with intra-IL or intra-PrL expression of ChR2, respectively. Inset, action potentials elicited by optogenetic stimulation.

(I and J) Diagrams and confocal images showing ChR2-expressing neural fibers in the NAcSh (I) and NAcCo (J) from rats with intra-IL or intra-PrL expression of ChR2.

(K) Example traces (left) and summarized results (right) showing that optogenetic stimulation (1 ms) of ChR2-expressing fibers in NAc slice from a rat with intra-IL or intra-PrL expression of ChR2 elicited synaptic currents at −70 mV in a NAcSh MSN that were inhibited by the AMPAR-selective antagonist NBQX (relative current in NBQX: IL-to-NAcSh, 7.1% ± 1.8%; t_4 = 50.6, p < 0.01; PrL-to-NAcCo, 5.6% ± 0.9%; t_4 = 102.1, p < 0.01).

(L) Example traces showing that currents from IL-to-NAcSh (left) or PrL-to-NAcCo (right) synapses exhibited short delays after presynaptic stimulation.

(M) Examples traces showing that currents from the IL-to-NAcSh (left) or PrL-to-NAcCo (right) synapses by optogenetic stimuli (1 ms stimulation duration) were prevented by TTX (1 μM).

(N) Example traces (left), trials (middle) of these traces, and summarized results (right) showing that the success rate of synaptic responses was decreased by TTX at both IL-to-NAcSh (t_5 = 10.5, p < 0.01, paired t test) and PrL-to-NAcCo (t_6 = 7.6, p < 0.01, paired t test) synapses.

(O) Example traces (left), trials of these traces (middle), and summarized results (right) showing that reducing the bath concentration of Ca^{2+} (from 2.5 to 1.0 mM) reduced the success rate of IL-to-NAcSh (t_4 = 4.3, p = 0.01, paired t test) and PrL-to-NAcCo (t_4 = 8.5, p < 0.01, paired t test) synapses.

(P) Example EPSCs (upper) and summarized results (lower) showing that optogenetic stimulation of the PrL projection elicited substantially larger responses in NAcCo neurons, whereas stimulation of the IL projection elicited substantially larger responses in NAcSh neurons ($F_{1,65}$ = 60.0, p < 0.01, two-way ANOVA; p < 0.01, NAcCo versus NAcSh for either PrL or IL, Bonferroni posttest).*p < 0.05; **p < 0.01.

induced responses in more detail. Both IL-to-NAcSh and PrL-to-NAcCo transmissions were prevented by perfusion of TTX (1 μM), indicating that the 1 ms optogenetic stimulation-elicited mPFC-to-NAc synaptic responses are action potential dependent (relative amplitude after TTX: IL-to-NAcSh, 8.4% ± 3.6%, n = 5, t_4 = 25.5, p < 0.01; PrL-to-NAcCo, 8.2% ± 3.0%, n = 5, t_4 = 30.2, p < 0.01; paired t test; Figure 1M). Notably, optogenetic stimulation with longer pulse durations may generate TTX-insensitive synaptic responses (Figures S1D–S1F). Importantly, the TTX-sensitive synaptic transmission was also evident when EPSCs were induced by minimal optogenetic stimulations, in which the laser duration was further decreased to 0.01–0.1 ms. Specifically, when the stimulation intensity/duration was reduced to the point at which successes and failures of synaptic transmission were induced alternatively, the success rate reflects (but is not necessarily equal to) the presynaptic release probability (Pr). The success rate at both IL-to-NAcSh and PrL-to-NAcCo synapses was reduced close to 0 by TTX (1 μM) (Figure 1N), and also substantially decreased when the extracellular concentration of Ca^{2+} was reduced (from 2.5 to 1.0 mM) (Figure 1O). Thus, minimal stimulation-induced EPSCs at IL-to-NAcSh and PrL-to-NAcCo synapses were likely triggered by action potential-dependent activation of voltage-gated calcium channels and the resulting calcium influx, similar to endogenous processes.

To examine whether the biophysical properties of optogenetically elicited EPSCs are consistent with electrically induced EPSCs, we performed the multiple-probability fluctuation analysis (MPFA) (Scheuss and Neher, 2001; Silver, 2003) in our optogenetic setup. We optically induced five consecutive EPSCs from IL-to-NAcSh or PrL-to-NAcCo synapses, and based on the relationship between the variance and the mean EPSC amplitudes (Figures S1I–S1M) (Suska et al., 2013), the estimated presynaptic release probability (Pr) was 0.55 ± 0.07 (n = 5) at IL-to-NAcSh synapses and 0.38 ± 0.10 (n = 5) at PrL-to-NAcCo synapses, consistent with the Pr (~0.4) of corticoaccumbens synapses estimated using electrical stimulation (Casassus et al., 2005) or other short-duration optogenetic stimulations (Suska et al., 2013). The Pr was much higher when EPSCs were elicited by optogenetic stimulation with long durations (Figure S1M). Finally, we examined the preferential projections of the IL and PrL to NAcSh and NAcCo using the optogenetic approach. In brain slices from rats with IL expression of ChR2, the same optogenetic stimulations induced much larger synaptic responses in NAcSh than in NAcCo, whereas in brain slices from rats with PrL expression of ChR2, the same optogenetic stimulations elicited much larger synaptic responses in NAcCo than NAcSh (Figure 1P). These results, together with the above anatomical results, suggest that in the rat, our optogenetic and physiological approaches can selectively target the IL and PrL projections to the NAcSh and NAcCo, respectively.

Cocaine Self-Administration Generates Silent Synapses in IL-to-NAcSh Projection

With the optogenetic stimulation procedures verified above, we performed the minimal stimulation assay (Huang et al., 2009; Isaac et al., 1995; Lee et al., 2013; Liao et al., 1995) to assess silent synapses within the IL-to-NAcSh projection during early withdrawal (1 day) from cocaine self-administration. We injected rats with ChR2-expressing AAV2 into the IL and trained them to nose-poke for intravenous cocaine for 6 days (one overnight session followed by 2 hr/day for 5 days at 0.75 mg/kg/infusion; infusions were paired with a light cue). As previously demonstrated (Lee et al., 2013), this training procedure induced progressive increases in cue-induced cocaine seeking after withdrawal (incubation of cocaine craving) with significantly higher nose-poke responding in extinction tests performed after 45 withdrawal days than after 1 day (Figures 2A and 2B). During the extinction tests, nose-poke responding led to light cue presentation, but not cocaine. On withdrawal day 1 (without extinction tests), we used the optogenetic minimal stimulation assay to assess the level (%) of silent synapses on NAcSh MSNs in saline- and cocaine-exposed rats. Specifically, minimal stimulations either induced or failed to induce small EPSCs at +50 or −70 mV. If AMPAR-silent synapses are present in a set of recorded synapses, the failure rate at −70 mV should be higher than that at +50 mV; based on these differential failure rates, the percentage of silent synapses among all synapses can be estimated (Liao et al., 1995). Our results show that the level of silent synapses within the IL-to-NAcSh projection was increased on withdrawal day 1 (Figures 2C–2E and S2A).

Maturation of Silent Synapses within the IL-to-NAcSh Projection after Prolonged Withdrawal

After 42–47 withdrawal days (referred to as 45 days hereafter), the level of silent synapses within the IL-to-NAcSh projection returned to the basal (saline) levels (Figures 2F–2H and S2B). We previously demonstrated that cocaine-generated silent synapses within the amygdala-to-NAc projection disappear by an unsilencing process involving recruitment of calcium-permeable AMPARs (CP-AMPARs) (Lee et al., 2013), key substrates in incubation of cocaine craving (Conrad et al., 2008; Wolf and Tseng, 2012). We tested whether cocaine-generated silent synapses within the IL-to-NAcSh projection followed the same cellular course. After 45 withdrawal days, evoked EPSCs from IL-to-NAcSh synapses showed increased inward-rectification (Figures 2I–K and S2C) and increased sensitivity to the CP-AMPAR-selective antagonist Naspm (200 μM; Figures 2L–2N and S2D), suggesting synaptic insertion of CP-AMPARs. Note that the I–V curves of AMPAR EPSCs in each recorded neuron were calibrated with their reversal potentials to minimize the influence of liquid junction potentials and insufficient voltage control.

To examine whether these CP-AMPARs were indeed inserted into cocaine-generated silent synapses during the unsilencing/maturation process, we inhibited CP-AMPARs with Naspm (200 μM) in slices from rats 45 days after saline (control condition) or cocaine self-administration (Figure S2E). In the minimal stimulation assay, pharmacological inhibition of CP-AMPARs did not affect the failure rate of EPSCs at either −70 or +50 mV evoked from IL-to-NAcSh synapses in saline-exposed rats (Figures 3A–3C and 3G). In contrast, 45 days after cocaine self-administration, inhibition of CP-AMPARs significantly increased the failure rate of EPSCs at −70 mV, but not at +50 mV, suggesting that some IL-to-NAcSh synapses contained predominantly CP-AMPARs at this withdrawal time point (Figure 3D–3F and 3G). Assessment of percentage of silent synapses using these failure

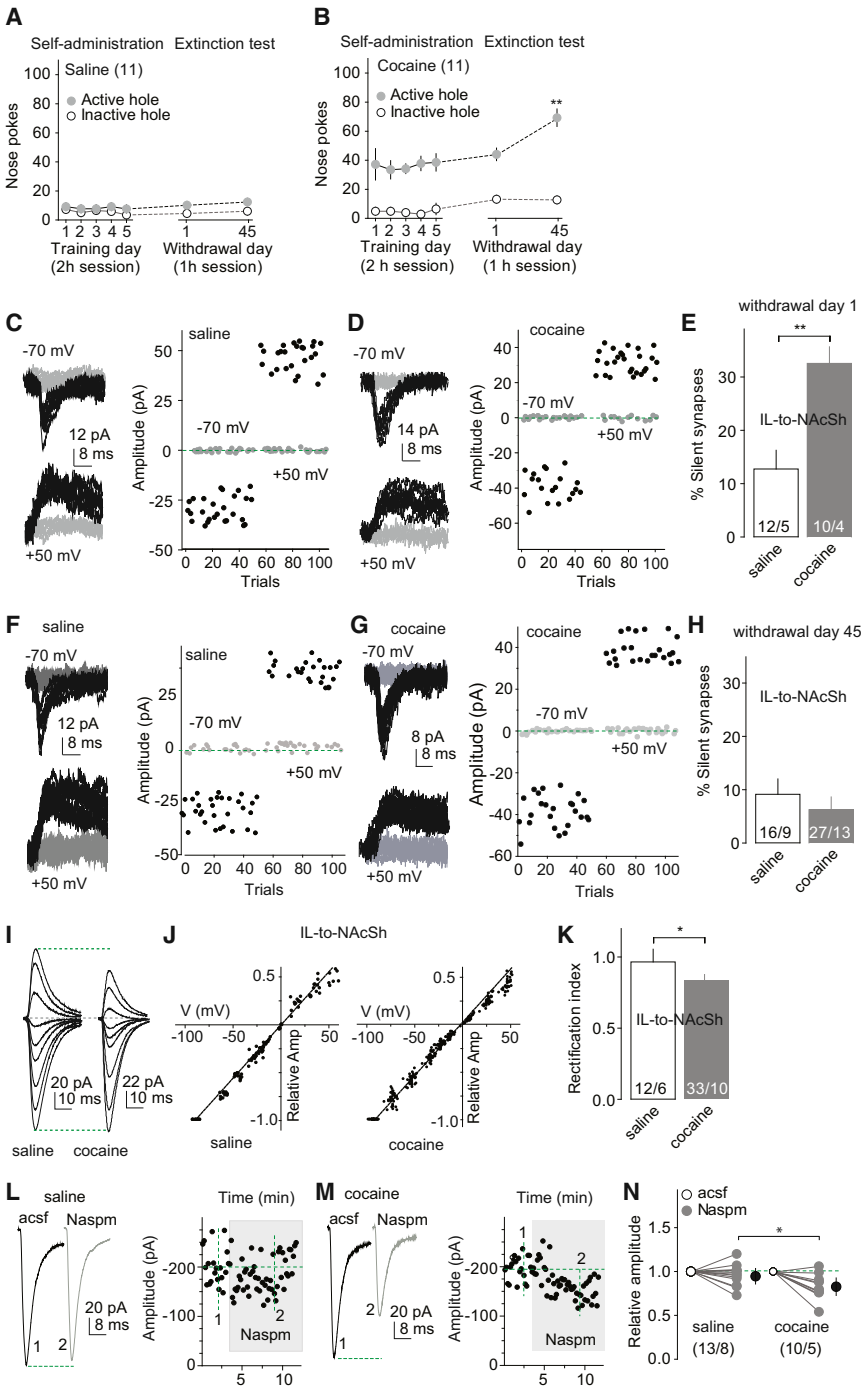

Figure 2. Generation and Maturation of Silent Synapses within the IL-to-NAcSh Projection after Cocaine Self-Administration

(A and B) Summarized results show that after saline (A) or cocaine (B) self-administration (2 hr session) for 5 days after ~12 hr overnight training cue-induced cocaine seeking (nose-pokes in the extinction test, 1 hr session) was significantly higher after 45 days of withdrawal from cocaine than after 1 day; nose-pokes remained low in all conditions in saline-exposed rats.

(C and D) EPSCs evoked at −70 or +50 mV by optogenetic minimal stimulation (left) over 100 trials (right) from an example recording of IL-to-NAcSh transmission 1 day after saline (C) or cocaine (D) self-administration.

(E) Summarized results showing that the level of silent synapses within the IL-to-NAcSh projection was significantly increased 1 day after cocaine self-administration (saline, 12.7% ± 3.5%, n/m = 12/5; cocaine, 32.5% ± 3.1%, n/m = 10/4; $t_{23} = 4.2$, $p < 0.01$, cell-based analysis, and $t_7 = 4.9$, $p < 0.01$, animal-based analysis).

(F and G) EPSCs evoked at −70 or +50 mV by optogenetic minimal stimulation (left) over 100 trials (right) from an example recording of IL-to-NAcSh transmission 45 days after saline (F) or cocaine (G) self-administration.

(H) Summarized results showing that the level of silent synapses within the IL-to-NAcSh projection in cocaine-exposed rats returned to the basal level (saline) after 45 withdrawal days (saline, 9.1% ± 2.9%, n/m = 16/9; cocaine, 6.3% ± 2.4%, n/m = 27/13; $t_{41} = 0.75$, $p = 0.46$, cell-based; $t_{20} = 1.3$, $p = 0.20$, animal-based, t test).

(I) Example EPSCs evoked from IL-to-NAcSh synapses at −70 to +70 mV (10–20 mV increments) from a saline- and a cocaine-exposed rat after 45 withdrawal days.

(J) The EPSC I-V curves from IL-to-NAcSh synapses in saline (left)-or cocaine (right)-exposed rats on withdrawal day 45.

(K) Summarized results showing that the rectification index of EPSCs from IL-to-NAcSh synapses was decreased (more rectifying) in cocaine-exposed rats on withdrawal day 45 (saline, 0.97 ± 0.09, n/m = 12/6; cocaine, 0.83 ± 0.01, n/m = 33/10; $t_{43} = 2.30$, $p = 0.03$, cell-based; $t_{14} = 2.6$, $p = 0.02$, animal-based, t test).

(L and M) Example EPSCs (left) and their time courses (right) from IL-to-NAcSh synapses in a saline-exposed (L) or cocaine-exposed (M) rat (on withdrawal day 45) before and during perfusion of Naspm.

(N) Summarized results showing that EPSCs from IL-to-NAcSh synapses were not affected by Naspm in saline-exposed rats, but were significantly inhibited by Naspm in cocaine-exposed rats (cell-based: saline/cocaine × acsf/Naspm, $F_{1,21} = 5.0$, $p = 0.04$, two-way ANOVA; $p < 0.01$, saline-Naspm versus cocaine-Naspm, Bonferroni posttest; animal-based: $F_{1,11} = 6.2$, $p = 0.03$). *$p < 0.05$; **$p < 0.01$.

rates showed that inhibition of CP-AMPARs partially recovered silent synapses in cocaine-exposed rats toward the level observed on withdrawal day 1, suggesting that some cocaine-generated silent synapses within this projection became unsilenced by recruiting CP-AMPARs after withdrawal from cocaine (Figure 3H).

LTD Reverses Maturation of Silent Synapses in the IL-to-NAcSh Projection

Synaptic insertion of CP-AMPARs in NAc is a prominent cellular adaptation involved in incubation of cocaine craving (Conrad et al., 2008). Compared to pre-existing AMPARs, newly inserted CP-AMPARs after withdrawal from cocaine may be loosely

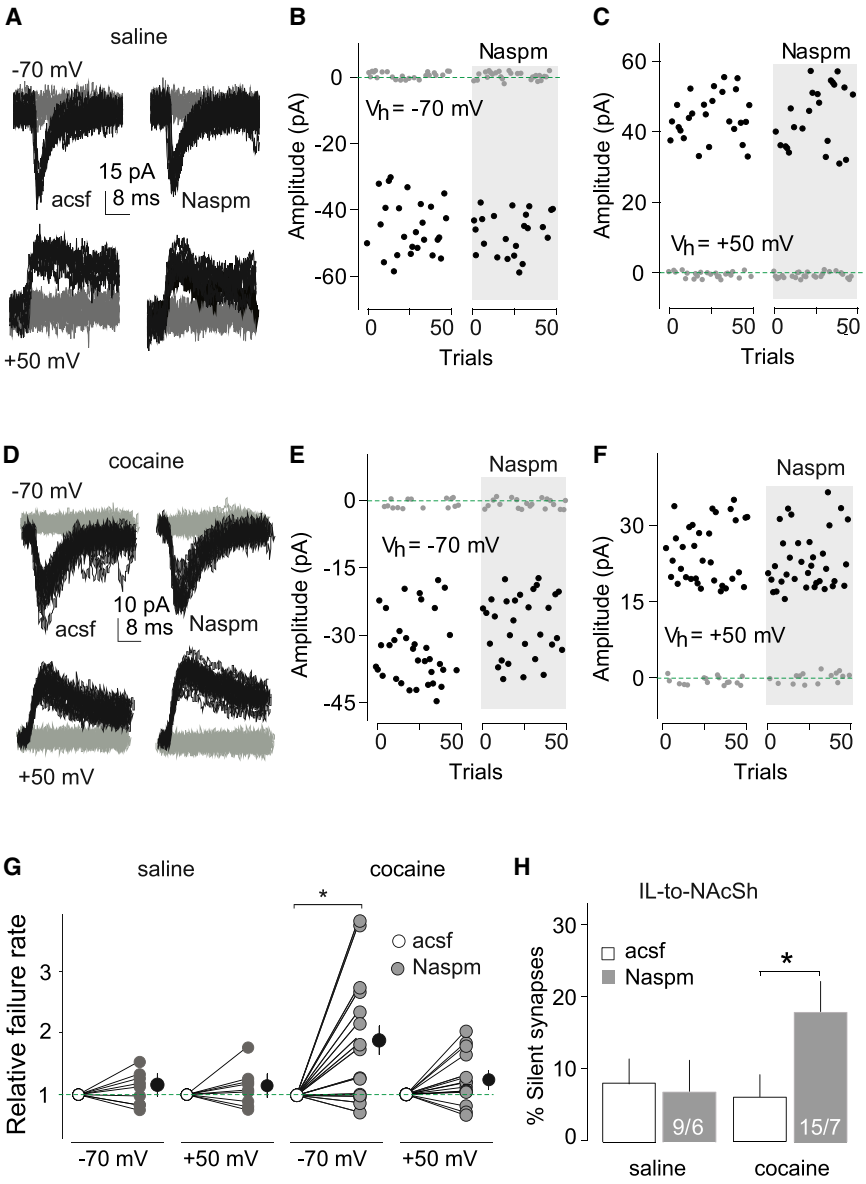

Figure 3. Inhibition of CP-AMPARs Causes Re-Emergence of Silent Synapses within the IL-to-NAcSh Projection after 45 days of Withdrawal from Cocaine

All experiments were performed using rats with intra-IL expression of ChR2 45 days after saline or cocaine self-administration.

(A) Example EPSCs evoked at −70 or +50 mV by optogenetic minimal stimulation of IL-to-NAcSh synapses in a saline-exposed rat before and during perfusion of Naspm.

(B and C) Consecutive trials of the example EPSCs in (A) at −70 (B) or +50 mV (C).

(D) Example EPSCs evoked at −70 or +50 mV by optogenetic minimal stimulation of IL-to-NAcSh synapses in a cocaine-exposed rat before and during perfusion of Naspm.

(E and F) Consecutive trials of the example EPSCs in (D) at −70 (E) or +50 mV (F).

(G) Summarized results showing that in saline-exposed rats the failure rate of IL-to-NAcSh synaptic transmission was not changed at either −70 or +50 mV by perfusion of Naspm (−70 mV/+50 mV × control-acsf/Naspm: $F_{1,16}$ = 0.01, p = 0.9, cell based; $F_{1,10}$ = 0.3, p = 0.60, animal based; two-way ANOVA). In cocaine-exposed rats, the failure rate was significantly increased by perfusion of Naspm at −70 mV, but not at +50 mV (cell based: −70 mV/+50 mV × control-acsf/Naspm, $F_{1,28}$ = 5.3, p = 0.03; two-way ANOVA; p < 0.01, control-acsf versus Naspm at −70 mV, Bonferroni posttest; animal based: $F_{1,12}$ = 7.9, p = 0.02).

(H) Summarized results showing that inhibiting CP-AMPARs by Naspm caused re-emergence of silent synapses within the IL-to-NAcSh projection 45 days after cocaine self-administration (cell based: saline-control, 9.4% ± 3.6%, saline-Naspm, 6.9% ± 4.5%, n/m = 9/6; cocaine-control, 6.4% ± 3.3%, cocaine-Naspm, 18.3% ± 4.3%, n/m = 15/7; saline/cocaine × control/Naspm, $F_{1,22}$ = 4.3, p = 0.04, two-way ANOVA; p = 0.02, cocaine control versus cocaine-Naspm, Bonferroni posttest; animal-based: $F_{1,11}$ = 9.5, p = 0.01). *p < 0.05.

tethered to the postsynaptic density and thus highly susceptible to regulation (Ferrario et al., 2011; McCutcheon et al., 2011). Some forms of long-term depression (LTD) of excitatory synaptic transmission, which are often achieved by internalization of synaptic AMPARs (Malenka and Bear, 2004), can be used to selectively internalize newly inserted CP-AMPARs.

We optimized an optogenetic LTD induction protocol (1 Hz × 10 min with pulse duration of 1 ms), which only induced LTD at IL-to-NAcSh synapses in slices from cocaine-exposed rats after 45 withdrawal days, but did not affect those synapses in saline-exposed rats (Figures 4A, 4B, and S2F). We selected a moderate LTD protocol so that the basal IL-to-NAcSh transmission would remain intact (i.e., no effect in saline controls) while cocaine-induced alterations were selectively manipulated. This LTD was prevented by pharmacological inhibition of metabotropic glutamate receptor 1 (mGluR1) by LY367385 (50 μM) or NMDARs by D-APV (50 μM) (Figures 4C and S2G), consistent with mGluR1's role as a negative regulator of CP-AMPARs and incubation (Loweth et al., 2014; Wolf and Tseng, 2012) and the established role of NMDARs in NAc LTD (Kasanetz et al., 2010). In saline-exposed rats, EPSCs at IL-to-NAcSh synapses were insensitive to Naspm (Figures 2L and 2N), and LTD induction did not change this sensitivity (Figures 4D, 4F, and S2F). In cocaine-exposed rats, EPSCs at IL-to-NAcSh synapses, which were sensitive to Naspm (Figures 2M and 2N), were no longer Naspm sensitive after LTD (Figures 4E, 4F, and S2F), indicating that our LTD protocol preferentially internalized/inhibited CP-AMPARs. Because CP-AMPARs are preferentially recruited to silent synapses after withdrawal from cocaine (Figures 2 and 3), this LTD protocol can be used to re-silence the newly matured/unsilenced synapses within the IL-to-NAcSh projection.

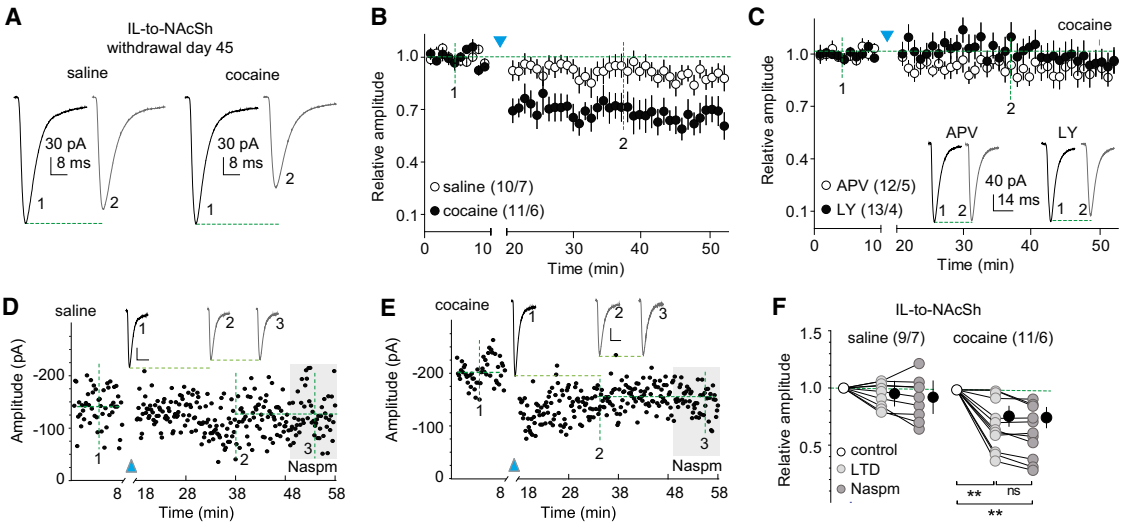

Figure 4. LTD Reverses Maturation of Silent Synapses within the IL-to-NAcSh Projection after 45 Days of Withdrawal from Cocaine

All experiments were performed using rats with intra-IL expression of ChR2 45 days after saline or cocaine self-administration.

(A) Example EPSCs from IL-to-NAcSh synapses before and after LTD induction in saline- or cocaine-exposed rats.

(B) Summarized results showing that the LTD induction did not affect IL-to-NAcSh transmission significantly in saline-exposed rats but induced LTD in cocaine-exposed rats (cell based: saline/cocaine × LTD time course: $F_{45,855} = 2.6$, $p < 0.01$, two-way ANOVA; $p = 1.00$, saline-preLTD [at data point indicated by "1"] versus saline-postLTD [at data point indicated by "2"]; $p < 0.01$, cocaine-preLTD [at "1"] versus cocaine-postLTD [at "2"], Bonferroni posttest; animal based: $F_{45,495} = 2.0$, $p < 0.01$).

(C) Summarized results showing that LTD induction within the IL-to-NAcSh projection in cocaine-exposed rats was prevented in the presence of either APV or LY (APV/LY × LTD time course: $F_{45,1035} = 1.0$, $p = 0.38$, cell based; $F_{45,315} = 1.2$, $p = 0.17$, animal based). Insets show an example EPSCs before and after LTD induction.

(D) Time course of EPSCs of an example recording of IL-to-NAcSh synapses in a saline-exposed rat before and after LTD induction, and during perfusion of Naspm after LTD. Inset shows averaged EPSCs taken around the time points as specified. Calibration bars, 30 pA, 10 ms.

(E) Time course of EPSCs of an example recording of IL-to-NAcSh synapses in a cocaine-exposed rat before and after LTD induction, and during perfusion of Naspm after LTD. Inset shows averaged EPSCs taken around the time points as specified. Calibration bars, 20 pA, 10 ms.

(F) Summarized results showing that in saline-exposed rats IL-to-NAcSh transmission was not affected by LTD induction and subsequent perfusion of Naspm ($F_{2,16} = 2.2$, $p = 0.15$, cell based; $F_{2,12} = 2.9$, $p = 0.09$, animal based, one-way ANOVA); in cocaine-exposed rats this transmission, which would be inhibited by Naspm, was no longer sensitive to Naspm after LTD induction (cell based: $F_{2,20} = 26.5$, $p < 0.01$, one-way ANOVA; $p < 0.01$, preLTD versus postLTD; $p < 0.01$, preLTD versus postLTD-Naspm; $p = 1.00$, postLTD versus postLTD-Naspm, Bonferroni posttest; animal based: $F_{2,10} = 18.2$, $p < 0.01$). **$p < 0.01$; ns, not significant.

Cocaine Self-Administration Generates Silent Synapses in the PrL-to-NAcCo Projection

Using similar experimental approaches, we selectively expressed ChR2 within the PrL (Figures 1E and 1H) and assessed silent synapses in the PrL-to-NAcCo projection 1 day after saline or cocaine self-administration (Figure S2H). As in IL-to-NAcSh projection, the level of silent synapses within the PrL-to-NAcCo was increased in cocaine-exposed, but not saline-exposed, rats (Figures 5A–5C).

Maturation of Silent Synapses within the PrL-to-NAcCo Projection after Prolonged Withdrawal from Cocaine

Within the PrL-to-NAcCo projection, the level of silent synapses also returned to the control level 45 days after withdrawal from cocaine (Figures 5D–5F and S2I). However, unlike the IL-to-NAcSh projection, EPSCs at PrL-to-NAcCo synapses did not show increased rectification (Figures 5G–5I and S2J) or increased Naspm (200 μM) sensitivity (Figures 5J–5L and S2K). Furthermore, on withdrawal day 45, perfusion of Naspm had no effect on the failure rates of minimal stimulation-evoked EPSCs within the PrL-to-NAcCo projection at either −70 or +50 mV in saline- or cocaine-exposed rats (Figures 6A–6G and S2L) and did not restore cocaine-generated silent synapses (Figures 6H and S2L). Thus, the mechanisms that mediate the "disappearance" of silent synapses within the PrL-to-NAcCo projection are different from those in the IL-to-NAcSh projection. This disappearance could result from synaptic pruning, but the observation that the number of dendritic spines in the NAcCo is increased after prolonged withdrawal from cocaine (Robinson et al., 2001) suggests synaptogenesis rather than synaptic pruning as the critical mechanism. Alternatively, cocaine-generated silent synapses within the PrL-to-NAcCo projection could be unsilenced by recruiting non-CP-AMPARs. If so, induction of LTD should still internalize/inhibit those newly inserted non-CP-AMPARs to reverse their maturation.

LTD Reverses Maturation of Silent Synapses in PrL-to-NAcCo Projection

To explore whether cocaine-generated silent synapses within the PrL-to-NAcCo projection mature by recruiting non-CP-AMPARs and whether this potential maturation can be reversed, we applied the optogenetic LTD protocol (1 Hz × 10 min) to

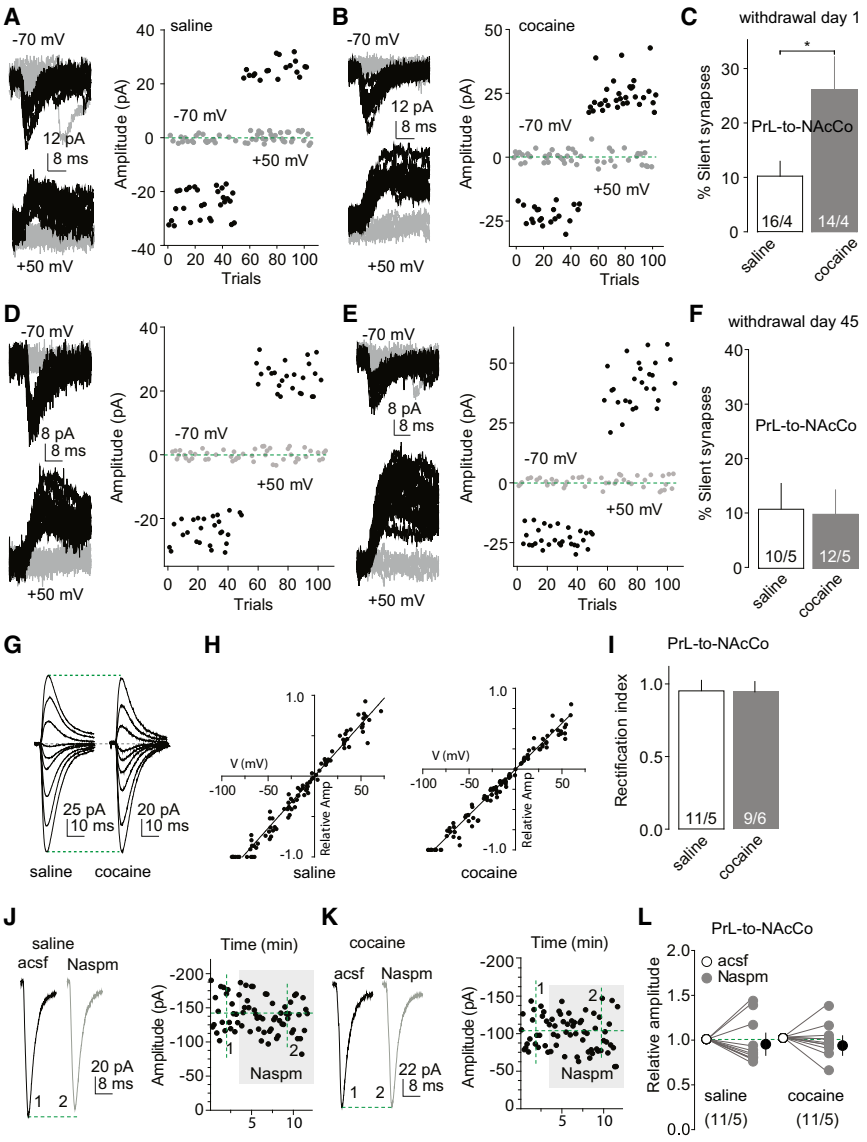

Figure 5. Generation and Maturation of Silent Synapses within the PrL-to-NAcCo Projection after Cocaine Self-Administration

(A and B) EPSCs evoked at −70 or +50 mV by optogenetic minimal stimulation (left) over 100 trials (right) from example recordings of PrL-to-NAcCo transmission in rats 1 day after saline (A) or cocaine (B) self-administration.

(C) Summarized results showing that percentage of silent synapses within the PrL-to-NAcCo projection was increased 1 day after cocaine self-administration (saline, 10.3% ± 2.8%, n/m = 16/4; cocaine, 26.2% ± 6.4%, n = 14/4; t_{28} = 2.4, p = 0.02, cell based; t_6 = 2.5, p = 0.04, animal based, t test).

(D and E) EPSCs evoked at −70 or +50 mV by optogenetic minimal stimulations (left) over 100 trials (right) from example recordings of PrL-to-NAcCo transmission in saline-exposed (D) or cocaine-exposed (E) rats 45 days after self-administration.

(F) Summarized results showing that percentage of silent synapses within the PrL-to-NAcCo projection in cocaine-exposed rats returned to the basal level (saline) after 45 withdrawal days (saline, 11.0% ± 4.9%, n/m = 10/5; cocaine, 10.2% ± 4.6%, n/m = 12/5; t_{20} = 0.13, p = 0.9, cell based; t_8 = 0.06, p = 0.95, animal based, t test).

(G) Example EPSCs evoked from PrL-to-NAcCo synapses at −70 to +70 mV (10–20 mV increments) from saline- and cocaine-exposed rats after 45 withdrawal days.

(H) The I–V curves of EPSCs evoked from PrL-to-NAcCo synapses in saline- or cocaine-exposed rats after 45 withdrawal days.

(I) Summarized results showing that rectification of AMPAR EPSCs from PrL-to-NAcCo synapses was not significantly altered in cocaine-exposed rats after 45 withdrawal days (saline, 0.96 ± 0.08, n/m = 11/5; cocaine, 0.96 ± 0.04, n/m = 9/6; t_{18} = 0.04, p = 0.97, cell based; t_9 = 0.8, p = 0.5, animal based, t test).

(J and K) Example EPSCs (left) and their time courses (right) from PrL-to-NAcCo synapses in a saline-exposed (J) or cocaine-exposed (K) rat before and during perfusion of Naspm.

(L) Summarized results showing that EPSCs from PrL-to-NAcCo synapses were not affected by Naspm in saline- or cocaine-exposed rats (saline/cocaine × control/Naspm: $F_{1,20} < 0.01$, p = 0.98, cell based; $F_{1,8}$ = 0.07, p = 0.79, animal based, two-way ANOVA). *p < 0.05.

PrL-to-NAcCo synapses in slices from rats 45 days after saline or cocaine self-administration (Figure S2M). Induction of LTD did not affect EPSCs in saline-exposed rats but induced depression of these synapses in cocaine-exposed rats (Figures 7A and 7B). Different from the induction mechanisms in the IL-to-NAcSh projection, LTD within the PrL-to-NAcCo projection in cocaine-exposed rats was prevented by application of the NMDAR antagonist D-APV, but not the mGluR1 antagonist LY367385 (Figures 7C and S2O). These results are consistent with the established role of mGluR1-dependent LTD, which preferentially targets synaptic CP-AMPARs in the NAc (Loweth et al., 2014). Thus, the LTD was likely achieved by NMDAR-dependent inhibition/internalization of non-CP-AMPARs.

As predicted, the expression of this LTD did not affect the sensitivity of EPSCs at PrL-to-NAcCo synapses to Naspm in saline- or cocaine-exposed rats (Figures 7D–7F and S2M). Importantly, induction of LTD induced re-emergence of silent synapses within the PrL-to-NAcCo synapses after 45 days of withdrawal from cocaine (Figures 7G–7L and S2N). These results suggest that cocaine-generated silent synapses within the PrL-to-NAcCo projection mature into fully functional synapses by recruiting non-CP-AMPARs, and LTD induction partially reverses this maturation. This appears to be a parsimonious interpretation, but other possibilities exist. For example, LTD induction may also silence some synapses that were not previously generated by cocaine exposure. In this case, behavioral consequences of LTD at PrL-to-NAcCo projection (see below) cannot be exclusively attributed to the reversal of silent synapse maturation. In either case, by generation and potential maturation of silent synapses, the IL-to-NAcSh and PrL-to-NAcCo

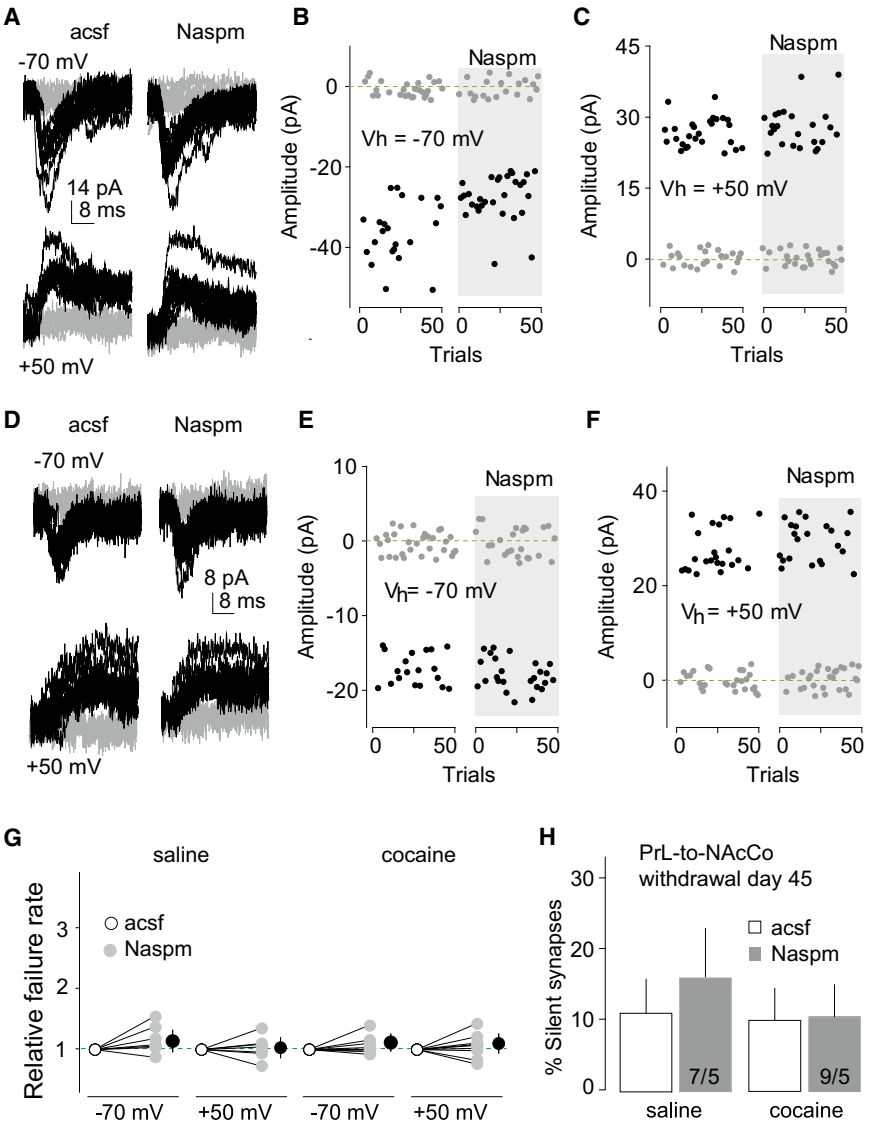

Figure 6. Inhibition of CP-AMPARs Does Not Cause Re-Emergence of Silent Synapses within the PrL-to-NAcCo Projection after 45 Days of Withdrawal from Cocaine

All experiments were performed using rats with PrL expression of ChR2 45 days after saline or cocaine self-administration.

(A) Example EPSCs evoked at −70 or +50 mV by optogenetic minimal stimulation of PrL-to-NAcCo synapses in a saline-exposed rat before and during perfusion of Naspm.

(B and C) Consecutive trials of the example EPSCs in (A) at −70 (B) or +50 mV (C).

(D) Example EPSCs evoked at −70 or +50 mV by optogenetic minimal stimulation of PrL-to-NAcCo synapses in a cocaine-exposed rat before and during perfusion of Naspm.

(E and F) Consecutive trials of the example EPSCs in (D) at −70 (E) or +50 mV (F).

(G) Summarized results showing that perfusion of Naspm did not affect the failure rates of PrL-to-NAcCo synaptic transmission at either −70 or +50 mV in saline-exposed (−70 mV/+50 mV × control-acsf/Naspm: $F_{1,12}$ = 1.4, p = 0.25, cell based; $F_{1,8}$ = 2.0, p = 0.20, animal based, two-way ANOVA) or cocaine-exposed (−70 mV/+50 mV × acsf/Naspm: $F_{1,16}$ < 0.01, p = 0.94, cell based; $F_{1,8}$ = 0.06, p = 0.81, animal based, two-way ANOVA) rats.

(H) Summarized results showing that inhibiting CP-AMPARs by Naspm did not cause re-emergence of silent synapses within the PrL-to-NAcCo projection 45 days after cocaine self-administration (percentage silent synapses: saline-control, 13.3 ± 6.6, saline-Naspm, 16.5 ± 7.8, n/m = 7/5; cocaine-control, 10.7 ± 5.8, cocaine-Naspm, 10.4 ± 4.6, n/m = 9/5; saline/cocaine × control/Naspm: $F_{1,14}$ = 0.08, p = 0.80, cell based; $F_{1,8}$ = 0.3, p = 0.61, animal based).

projections are simultaneously remodeled after withdrawal from cocaine.

Opposing Behavioral Effects of Silent Synapse-Based Remodeling of IL- and PrL-to-NAc Projections

The cocaine self-administration procedure that induced silent synapse-based circuitry remodeling led to incubation of cocaine craving (Figure 2B) (Lee et al., 2013), a process that may contribute to drug relapse in humans (Bedi et al., 2011). We next applied the established LTD protocol in vivo to examine the roles of silent synapse-based remodeling of these two mPFC-to-NAc projections in incubation of cocaine craving.

To manipulate the IL-to-NAcSh projection in vivo, we first verified the in vivo efficacy of the LTD protocol. Rats received IL injections of ChR2-expressing AAV2 and were implanted bilaterally with optical fibers in NAcSh. After cocaine self-administration and 45 withdrawal days, in vivo LTD was induced by optogenetic stimulation via preimplanted optical fibers (Figure 8A). We obtained brain slices from postinduction rats and observed that CP-AMPARs were no longer detectable at IL-to-NAcSh synapses (Figures 8B, 8C, and S3A), suggesting reversal of maturation of silent synapses, as demonstrated in vitro (Figure 4).

We then delivered this LTD protocol to cocaine-exposed rats on withdrawal day 45 and ~1 min later assessed cue-induced cocaine seeking in the extinction test (1 hr). We found that reversing the maturation of cocaine-generated silent synapses within the IL-to-NAcSh projection *enhanced* cue-induced cocaine seeking (Figures 8D, S3C, and S3E). These results suggest that silent synapse-based remodeling of the IL-to-NAcSh projection normally inhibits cue-induced cocaine seeking, and that interfering with this inhibition results in increased cocaine seeking.

To manipulate the PrL-to-NAcCo projection, we again first verified the in vivo efficacy of the LTD protocol. Specifically,

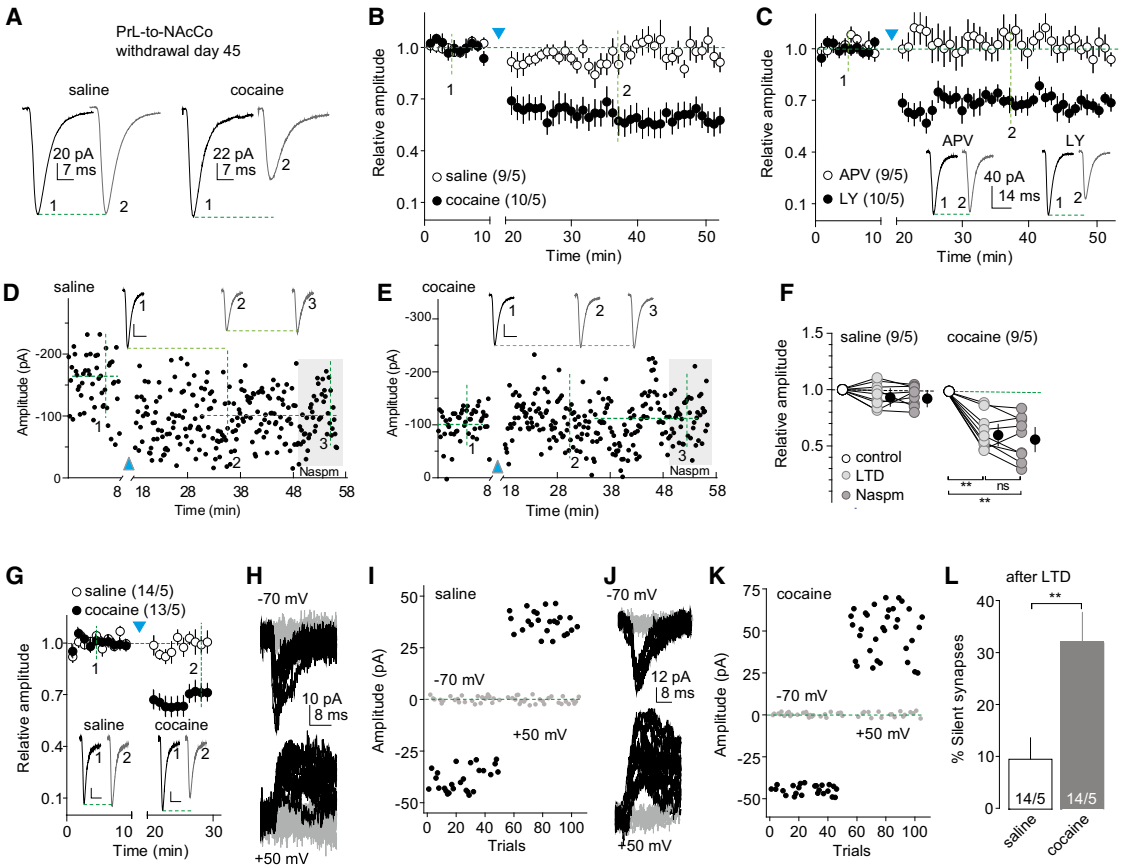

Figure 7. LTD Reverses Maturation of Silent Synapses within the PrL-to-NAcCo Projection after 45 Days of Withdrawal from Cocaine

All experiments were performed using rats with intra-PrL expression of ChR2 45 days after saline or cocaine self-administration.

(A) Example EPSCs from PrL-to-NAcCo synapses before and after LTD induction in saline- or cocaine-exposed rats.

(B) Summarized results showing that the LTD induction did not affect PrL-to-NAcCo transmission in saline-exposed rats, but induced LTD in cocaine-exposed rats (saline/cocaine × pre/postLTD: $F_{45,765} = 6.2$, $p < 0.01$, two-way ANOVA; $p = 0.99$, saline-preLTD [at "1"] versus saline-postLTD [at "2"]; $p < 0.01$, cocaine-preLTD [at "1"] versus cocaine-postLTD [at "2"], Bonferroni posttest, cell based; $F_{45,360} = 6.1$, $p < 0.01$, animal based).

(C) Summarized results showing that LTD expression within the PrL-to-NAcCo projection in cocaine-exposed rats was prevented in the presence of APV but not LY (APV/LY × LTD time course: $F_{45,765} = 4.4$, $p < 0.01$, two-way ANOVA; $p = 1.00$, control versus APV at "2"; $p = 0.01$, control-LY versus LTD-LY at "2," Bonferroni posttest, cell based; $F_{45,360} = 4.0$, $p < 0.01$, animal based). Insets show example EPSCs before and after LTD induction.

(D) Time course of EPSCs of an example recording of PrL-to-NAcCo synapses in a saline-exposed rat before and after LTD induction, and during perfusion of Naspm after LTD. Inset shows averaged EPSCs taken around the time points as specified. Calibration bars, 25 pA, 10 ms.

(E) Time course of EPSCs of an example recording of PrL-to-NAcCo synapses in a cocaine-exposed rat before and after LTD induction, and during perfusion of Naspm after LTD. Inset shows averaged EPSCs taken around the time points as specified. Calibration bars, 20 pA, 10 ms.

(F) Summarized results showing that EPSCs from PrL-to-NAcCo synapses were not affected by LTD protocol in saline-exposed rats ($F_{2,16} = 1.7$, $p = 0.22$, cell-based; $F_{2,8} = 2.61$, $p = 0.13$, animal-based; one-way ANOVA,) but were decreased in cocaine-exposed rats ($F_{2,16} = 35.1$, $p < 0.01$, one-way ANOVA; $p < 0.01$, preLTD versus either postLTD or postLTD-Naspm; $p = 0.84$, postLTD versus postLTD-Naspm, Bonferroni posttests, cell based; $F_{2,8} = 31.87$, $p < 0.01$, animal based), and perfusion of Naspm after LTD did not induce additional changes in EPSCs in either saline- or cocaine-exposed rats.

(G) Summarized results showing the LTD induction of two sets of NAcCo MSNs (from saline- or cocaine-exposed rats) that were subsequently assessed for percentage of silent synapse analysis in (H)–(L). Inset shows EPSCs from PrL-to-NAcCo synapses before and after LTD induction in saline- or cocaine-exposed rats (saline/cocaine × LTD time course: $F_{19,475} = 9.3$, $p < 0.01$, cell based; $F_{(19,152)} = 5.9$, $p < 0.01$, animal based; two-way ANOVA). Calibration bars, 30 pA, 10 ms.

(H and I) EPSCs evoked at −70 or +50 mV by optogenetic minimal stimulations (H) over 100 trials (I) in an example recording of PrL-to-NAcCo synapses after LTD induction of these synapses in a saline-exposed rat.

(J and K) EPSCs evoked at −70 or +50 mV by optogenetic minimal stimulations (J) over 100 trials (K) in an example recording of PrL-to-NAcCo synapses after LTD induction of these synapses in a cocaine-exposed rat.

(L) Summarized results showing that LTD induction induced reemergence of silent synapses in the PrL-to-NAcCo projection of rats 45 days after cocaine self-administration (percentage of silent synapses: saline, 9.8 ± 4.2, n/m = 14/5; cocaine, 32.4 ± 6.2, n/m = 14/5, $t_{26} = 3.04$, $p < 0.01$, t test, cell based; $t_8 = 2.5$, $p = 0.04$, animal based). **$p < 0.01$; ns, not significant.

after 45 withdrawal days, the LTD induction protocol was applied by optogenetic stimulation to the NAcCo in rats with PrL expression of ChR2. We then obtained the brain slices and observed that the percentage of silent synapses within the PrL-to-NAcCo projection was partially restored in cocaine-exposed rats receiving LTD induction (Figures 8E–8I and S3B),

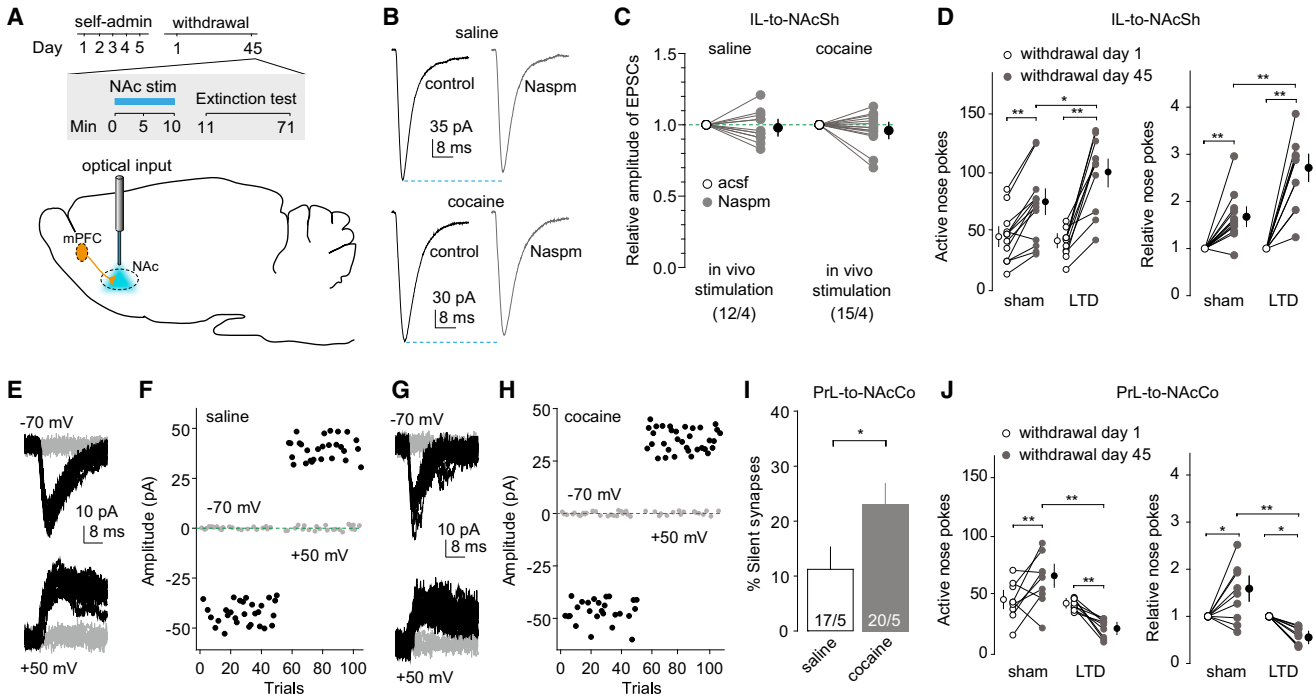

Figure 8. Reversing the Maturation of Silent Synapses in the IL-to-NAcSh and PrL-to-NAcCo Projections Causes Opposing Effects on Incubation of Cocaine Craving

(A) Diagrams showing the timeline of behavioral experiments and the LTD induction in both PFC-to-NAc projections before the test for cue-induced cocaine seeking on withdrawal day 45.

(B) Example EPSCs from IL-to-NAcSh synapses before and during perfusion of Naspm in a NAc slice from a rat receiving intra-NAcSh LTD induction 45 days after saline (upper) or cocaine self-administration (lower).

(C) Summarized results showing that in cocaine-exposed rats EPSCs at IL-to-NAcSh synapses were no longer inhibited by Naspm after in vivo LTD induction (saline/cocaine × withdrawal day: $F_{1,25} = 0.16$, $p = 0.69$, cell based; $F_{1,6} = 0.00$, $p = 0.95$, animal based; two-way ANOVA).

(D) LTD induction in the IL-to-NAcSh projection increased incubated cue-induced cocaine seeking in the extinction test. Data are presented as the numbers of nose-pokes to active holes on withdrawal days 1 and 45 (left) (withdrawal day × sham/LTD: $F_{1,22} = 13.4$, $p < 0.01$, two-way ANOVA; $p < 0.01$, sham-withdrawal day 1 versus sham-withdrawal day 45; $p = 0.01$, sham-withdrawal day 45 versus LTD-withdrawal day 45, Bonferroni posttest) and the nose-pokes on withdrawal day 45 relative to withdrawal day 1 (right) (withdrawal day × sham/LTD: $F_{1,22} = 13.1$, $p < 0.01$, two-way ANOVA; $p < 0.01$, sham-withdrawal day 1 versus sham-withdrawal day 45; $p < 0.01$, sham-withdrawal day 45 versus LTD-withdrawal day 45, Bonferroni posttest).

(E–H) Example EPSCs and their time courses in the minimal stimulation assay of PrL-to-NAcCo projection in a NAc slice from a rat receiving intra-NAcCo LTD induction 45 days after saline (E and F) or cocaine (G and H) self-administration.

(I) Summarized results showing that after in vivo LTD induction in the PrL-to-NAcCo projection, percentage of silent synapses was increased 45 days after cocaine self-administration (saline, 11.2% ± 4.3%, n/m = 17/5; cocaine, 23.2% ± 4.9%, n/m = 20/5, $t_{35} = 2.0$, $p = 0.048$, cell based; $t_8 = 3.3$, $p = 0.01$, anima based; t test).

(J) LTD induction in the PrL-to-NAcCo projection decreased incubated cue-induced cocaine seeking in the extinction test. Data are presented as the numbers of nose-pokes to active holes on withdrawal days 1 and 45 (left) (withdrawal day × sham/LTD: $F_{1,16} = 17.8$, $p < 0.01$, two-way ANOVA; $p < 0.01$, sham-withdrawal day 1 versus sham-withdrawal day 45; $p < 0.01$, LTD-withdrawal day 1 versus LTD-withdrawal day 45; $p < 0.01$, sham-withdrawal day 45 versus LTD-withdrawal day 45, Bonferroni posttest) and changes (relative) of nose-pokes between the two withdrawal days (right) (withdrawal day × sham/LTD: $F_{1,16} = 16.9$, $p < 0.01$, two-way ANOVA; $p = 0.03$, sham-withdrawal day 1 versus sham-withdrawal day 45; $p = 0.02$, LTD-withdrawal day 1 versus LTD-withdrawal day 45; $p < 0.01$, sham-withdrawal day 45 versus LTD-withdrawal day 45, Bonferroni posttest). *$p < 0.05$; **$p < 0.01$.

suggesting a reversal of maturation of silent synapses. In another group of rats with the same cocaine self-administration experience and stereotaxic surgeries, we applied the LTD induction protocol to PrL-to-NAcCo projections on withdrawal day 45, followed by an extinction test. Reversing maturation of cocaine-generated silent synapses within the PrL-to-NAcCo projection *decreased* cue-induced cocaine seeking to a level even lower than that observed on withdrawal day 1 (Figures 8J, S3D, and S3E). The additional reduction likely reflects a general role of this projection in cue-induced cocaine seeking (See, 2005), independent of the withdrawal period. For example, some pre-existing synapses within this projection may become AMPAR silent upon LTD induction, resulting in additional weakening of this projection, thus lowering cocaine seeking. Furthermore, it is unlikely that the inhibitory effect of LTD stimulation on nose-poke responding in the extinction test is due to motor impairments. We found that in vivo LTD induction had no effect on high rate operant responding in rats trained to nose-poke for sucrose reward (Figure S3F). Overall, in contrast to the IL-to-NAcSh projection, silent synapse-based remodeling of PrL-to-NAcCo projection functions to promote incubation of cocaine craving.

DISCUSSION

Our results show that the two primary mPFC projections underwent silent synapse-based remodeling after withdrawal from cocaine self-administration, and that disruption of the remodeling of these projections resulted in opposite effects on incubation of cocaine craving (Figure S4). Importantly, the two projections underwent different forms of silent synapse-based remodeling that involved CP-AMPARs in IL-to-NAcSh and non-CP-AMPARs in PrL-to-NAcCo.

Silent Synapse-Based Circuitry Remodeling after Withdrawal from Cocaine Self-Administration

Synaptic connections are the core components determining the anatomical and functional properties of neural circuits and consequently learned behaviors and motivational states. Under normal conditions, the NAc circuits are assumed to remain relatively stable in order to maintain stable and reversible emotional and motivational states (Mogenson and Yang, 1991).

One way to redefine the circuitry architecture is through generation of new synaptic contacts. In the NAc, exposure to cocaine generates silent synapses that possess key features of nascent glutamatergic synapses (Brown et al., 2011; Huang et al., 2009); in parallel, there may be an increase in the number of dendritic spines (Robinson et al., 2001) and activation of prosynaptogenesis transcriptional and neurotrophic cascades (Chao and Nestler, 2004; Koya et al., 2012). These results led to the idea that cocaine-generated silent synapses are nascent synaptic contacts, and that generation and maturation of silent synapses remodel the NAc glutamatergic circuits and redefine the related information flow that controls cocaine-taking behaviors (Dong and Nestler, 2014; Huang et al., 2013). Guided by this idea, our goal here was to interfere with these cocaine induced, potentially new synaptic contacts in the mPFC-to-NAc projections, without interfering with basal pre-existing synaptic transmission in these projections. To achieve this goal, we chose a modest LTD induction protocol (1 Hz × 10min with pulse duration of $\leq$1 ms). This LTD protocol removed CP-AMPARs in cocaine-exposed rats but did not affect IL-to-NAc synaptic transmission in saline-exposed rats (Figures 4A, 4B, 7A, and 7B), suggesting selective disruption/interference of cocaine-induced silent synapses.

A potential concern with this interpretation is raised by previous work demonstrating broad upregulation of NAc CP-AMPARs after withdrawal from a longer-access cocaine self-administration regimen (Wolf and Tseng, 2012). If our cocaine self-administration regimen leads to CP-AMPAR incorporation into pre-existing synapses in addition to silent synapses, and our LTD protocol induces AMPAR internalization at both types of synapses, the LTD protocol would not only result in reversal of maturation of silent synapses but would also induce a more generalized depression of PFC-to-NAc synapses. However, arguing against this possibility, our further analysis suggests that LTD-induced internalization of AMPARs from pre-existing IL-to-NAcSh synapses was minimal. As demonstrated in Figure 3, the basal level of silent synapses was ~7% within the IL-to-NAcSh projection after 45 withdrawal days, and was recovered to ~18% upon CP-AMPAR inhibition (Figure 3H). Thus, ~11% of IL-to-NAcSh synapses were CP-AMPAR-containing, matured silent synapses at this withdrawal time point. At the single-channel level, GluA2-lacking CP-AMPARs exhibit ~4-fold (8.7 versus 2.2 pS) higher conductance at negative membrane potentials (i.e., −70 mV) than regular AMPARs (Ozawa et al., 1991). Factoring in this consideration, contribution of these 11% matured silent synapses to total EPSCs should be ~33% (estimated as [11% × 4]/[11% × 4 + 89% × 1] = 0.33). After LTD induction, the amplitude of total EPSCs was decreased by ~30% (Figure 4B). Combined with the observation that the Naspm sensitivity was not observed after LTD induction, it is likely that the CP-AMPAR-containing, matured silent synapses were the primary targets of our LTD manipulation.

IL-to-NAcSh, BLA-to-NAcSh, and PrL-to-NAcCo Projections in Incubation of Cocaine Craving

Using region-specific pharmacological manipulations, recent studies show that the IL and NAcSh contribute to extinction-induced suppression of cocaine seeking (LaLumiere et al., 2012; Peters et al., 2008). A primary projection from the IL is to the NAcSh (Sesack et al., 1989), and our results show that one function of silent synapse-based remodeling of this projection is to inhibit incubation of cue-induced cocaine craving. These findings not only depict a circuitry-based antirelapse mechanism but also potentially clarify some complexities uncovered in prior studies of the circuitry of cocaine relapse.

First, although the NAcSh is essential for cocaine priming and cue-induced reinstatement after extinction (Bossert et al., 2013; Schmidt et al., 2005), inactivation of NAcSh can also reinstate cocaine seeking after extinction (Peters et al., 2008), suggesting dichotomous roles of NAcSh. Our previous and current results show that silent synapse-based remodeling of the BLA (Lee et al., 2013) and IL projections to the NAcSh (Figures 2 and 3) caused opposing effects on incubation of cocaine craving, indicating that the dichotomous roles of the NAcSh are likely to be achieved by different NAcSh afferents. It has been shown that excitatory projections from different brain regions arrive at different dendritic locations of NAc MSNs and possess different synaptic properties, often in a cell type (i.e., dopamine D1 versus D2 receptor-expressing MSNs)-specific manner (Britt et al., 2012; MacAskill et al., 2012). With such differential anatomical architectures, the remodeled IL and BLA projections may differentially reshape local circuits within NAcSh as well as NAcSh projections of the "direct" and "indirect pathways," resulting in differential or opposing behavioral consequences. Interestingly, a recent study shows that withdrawal from a different cocaine self-administration regimen in mice selectively induces synaptic insertion of CP-AMPARs in the mPFC projection to D1-expressing NAcSh neurons (Pascoli et al., 2014), highlighting the potential for circuit-specific as well as cocaine regimen-specific effects.

Second, it has been shown that pharmacologically inhibiting the IL decreases incubation of cocaine craving (Koya et al., 2009). Furthermore, selective inactivation of cFos-expressing IL neurons inhibits context-induced reinstatement of heroin seeking (Bossert et al., 2011), as does anatomical "disconnection" of the IL-to-NAcSh projection (Bossert et al., 2012). These seemingly discrepant results may indicate a complex nature of

the IL-to-NAcSh projection in the control of drug seeking. One scenario is that the basal, pre-existing function of IL-to-NAcSh projection is required for establishing cue- or context-induced relapse to drug seeking, but this projection acquires new antirelapse functions after withdrawal from cocaine. Manipulations in these previous studies may differentially affect the pre-existing and acquired functions of this projection. In our study, we selectively targeted the cocaine-induced silent synapses without affecting basal drug-naive glutamatergic transmission. This more-selective in vivo optogenetic LTD protocol, which interfered with these new synapses in this projection rather than disrupting pre-existing synapses, promoted the expression of incubation of cocaine craving (Figure 8D).

Third, in contrast to the IL-to-NAcSh projection, reversing maturation of PrL-to-NAcCo silent synapses on withdrawal day 45 decreased incubation of cocaine craving (Figure 8J). This result is in agreement with previous findings indicating that prior cocaine self-administration increases PrL-to-NAcCo glutamatergic transmission induced by cocaine priming, and that inhibition of the PrL-to-NAcCo projection inhibits reinstatement of cocaine seeking (McFarland et al., 2003; Stefanik et al., 2013). In addition to the PrL-to-NAcCo projection, maturation of silent synapses in the BLA-to-NAcSh is also essential for incubation of cocaine craving (Lee et al., 2013), suggesting a close connection between the BLA and PrL in modulating NAc-based cocaine-taking behaviors. Indeed, it has been observed that the BLA and mPFC projections gate each other's influences on NAc-based cellular and behavioral responses (Jackson and Moghaddam, 2001; McGinty and Grace, 2008), likely also involving the NAcCo and shell interactions. We speculate that the metastructure of the BLA and PrL projections to the NAc shell and core, as well as the shell-core interaction, are redefined following silent synapse-based remodeling of individual circuits, and the integrated effect mediates the incubation of cocaine craving.

NAc CP-AMPARs in Incubation of Cocaine Craving

Upregulation of NAc CP-AMPARs after withdrawal from extended access cocaine self-administration has been previously demonstrated as a critical mechanism of incubation of cocaine craving (Conrad et al., 2008; Loweth et al., 2014). On the other hand, cocaine self-administration followed by extinction training is also associated with AMPAR upregulation (Sutton et al., 2003), and overexpression of GluA1 in the NAc attenuates cocaine-induced (but not cue-induced) reinstatement of cocaine seeking after extinction (Bachtell et al., 2008).

Our results showing that the nature and behavioral consequences of cocaine-induced AMPAR upregulation are pathway specific may help explain these seemingly contradictory findings. Most strikingly, synaptic insertion of CP-AMPARs contributes to maturation of silent synapses in both BLA- (Lee et al., 2013) and IL-to-NAcSh projections (Figure 2) after withdrawal from cocaine, but CP-AMPAR accumulation within these two NAcSh afferents has opposite effects on incubation of cocaine craving. Furthermore, while the expression of incubation of cocaine craving after prolonged withdrawal depends on CP-AMPAR accumulation (Conrad et al., 2008; Loweth et al., 2014), recruitment of non-CP-AMPARs to PrL-to-NAcCo silent synapses after prolonged withdrawal (Figure 5) also promotes this incubation. Thus, multiple parallel mechanisms are likely induced simultaneously after cocaine self-administration to regulate glutamatergic transmission within the NAc, varying among different projections, withdrawal times, and durations of cocaine exposure. This raises questions for future studies, including whether other projections to NAc (e.g., ventral subiculum) also undergo silent synapse/CP-AMPAR-based remodeling and contribute to incubation of cocaine craving.

Concluding Remarks

Biology always goes with yin and yang, and our present results suggest that relapse—a key feature of addiction—is no exception. We showed that the two mPFC projections to the NAc both undergo silent synapse-based remodeling after cocaine self-administration but produce opposite effects on incubation of cocaine craving. Unveiling the endogenously triggered pro- and antirelapse circuitry remodeling may provide insight into ways to manipulate this yin-yang balance and hopefully to provide new neurobiological targets for interventions designed to decrease relapse to cocaine.

EXPERIMENTAL PROCEDURES

Detailed procedures are provided in the Supplemental Information.

Subjects

Male Sprague-Dawley rats (Charles River), postnatal day 28–30 at the beginning of the experiments were used. The rats were used in accordance with protocols approved by the Institutional Animal Care and Use Committees at the University of Pittsburgh and the European Neuroscience Institute.

Behavioral Studies

Drugs

Cocaine HCl was dissolved in 0.9% NaCl saline. Ketamine and xylazine were mixed for anesthesia. Pentobarbital sodium was purchased from DEA-designated vendor at the University of Pittsburgh.

Viral Delivery

A 26-gauge injection needle was used to bilaterally inject 1 μl/site (0.2 μl/min) of the AAV2 solution into the ventral (IL) (in mm, AP, +3.00; ML, ±0.70; DV, −4.75), or dorsal regions of the mPFC (PrL) (in mm, AP, +3.00; ML, ±0.75; DV, −4.00). Electrophysiological analyses were conducted ~3 (1 day withdrawal) or ~8 weeks (45 days withdrawal) after viral injection.

Self-Administration Surgery, Apparatus, and Training

Procedures are described in the Supplemental Information. Notably, the current cocaine self-administration procedure is slightly different from the one we previously used (Lee et al., 2013): (1) rats used in previous studies were purchased from Harlan, whereas rats used in the current studies were purchased from Charles River; and (2) in previous studies, a fixed volume of cocaine solution, and thus a fixed infusion duration, was used for each infusion. As such, the concentrations were adjusted by body weight during each training session. In the present study, the concentration of cocaine was fixed. As such, the infusion volume, and thus the infusion duration, varied during training sessions.

Optogenetic Procedures

For in vivo optical stimulation of mPFC projections, two 105 μm core optic fibers were modified for attachment to an internal cannula creating the optical neural interface (ONI) as described previously (Lee et al., 2013). Optic fiber light intensity was adjusted to ~10 mW of in vivo delivery of LTD protocols.

Electrophysiological Studies

Detailed procedures are provided in the Supplemental Information.

Data Acquisition and Analysis

In all electrophysiology experiments, data were coded before analysis. Data were then decoded for the final analysis. All results are shown as mean ± SEM. Sample size in electrophysiology experiments was presented as n/m, where "n" refers to the number of cells examined and "m" refers to the number of rats. Statistical significance was assessed using t test or one-way/two-way ANOVAs (with Bonferroni post tests). For all electrophysiology experiments involving treated rats, both cell- and animal-based statistics were performed and reported, with results of cell-based analysis provided in graphic presentations. In animal-based analyses, data of all recorded cells from a single rat were averaged, and the mean was used to represent this rat.

SUPPLEMENTAL INFORMATION

Supplemental Information includes Supplemental Experimental Procedures and four figures and can be found with this article at http://dx.doi.org/10.1016/j.neuron.2014.08.023.

ACKNOWLEDGMENTS

We thank Drs. Peter Kalivas and Peter Neumann for helpful comments on the manuscript. The reported work was supported by NIH intramural funds (Y.S.) and extramural funds DA028020 (B.R.L.), DA009621 (M.E.W.), DA015835 (M.E.W.), DA029565 (Y.H.H.), DA035805 (Y.H.H.), MH101147 (Y.H.H.), DA023206 (Y.D.), DA030379 (M.E.W. and Y.D.), DA034856 (Y.D.), the Pennsylvania Department of Health Commonwealth Universal Research Enhancement (Y.H.H.), NSFC 81328011 (R.C.), and the Deutsche Forschungsgemeinschaft through the Cluster of Excellence "Nanoscale Microscopy and Molecular Physiology of the Brain" (O.M.S.). The European Neuroscience Institute-Göttingen is jointly funded by the Max-Planck Society and University Medicine Göttingen. Cocaine was supplied by the Drug Supply Program of NIH NIDA.

Accepted: August 7, 2014
Published: September 4, 2014

REFERENCES

Bachtell, R.K., Choi, K.H., Simmons, D.L., Falcon, E., Monteggia, L.M., Neve, R.L., and Self, D.W. (2008). Role of GluR1 expression in nucleus accumbens neurons in cocaine sensitization and cocaine-seeking behavior. Eur. J. Neurosci. *27*, 2229–2240.

Bedi, G., Preston, K.L., Epstein, D.H., Heishman, S.J., Marrone, G.F., Shaham, Y., and de Wit, H. (2011). Incubation of cue-induced cigarette craving during abstinence in human smokers. Biol. Psychiatry *69*, 708–711.

Bossert, J.M., Stern, A.L., Theberge, F.R., Cifani, C., Koya, E., Hope, B.T., and Shaham, Y. (2011). Ventral medial prefrontal cortex neuronal ensembles mediate context-induced relapse to heroin. Nat. Neurosci. *14*, 420–422.

Bossert, J.M., Stern, A.L., Theberge, F.R., Marchant, N.J., Wang, H.L., Morales, M., and Shaham, Y. (2012). Role of projections from ventral medial prefrontal cortex to nucleus accumbens shell in context-induced reinstatement of heroin seeking. J. Neurosci. *32*, 4982–4991.

Bossert, J.M., Marchant, N.J., Calu, D.J., and Shaham, Y. (2013). The reinstatement model of drug relapse: recent neurobiological findings, emerging research topics, and translational research. Psychopharmacology (Berl.) *229*, 453–476.

Britt, J.P., Benaliouad, F., McDevitt, R.A., Stuber, G.D., Wise, R.A., and Bonci, A. (2012). Synaptic and behavioral profile of multiple glutamatergic inputs to the nucleus accumbens. Neuron *76*, 790–803.

Brog, J.S., Salyapongse, A., Deutch, A.Y., and Zahm, D.S. (1993). The patterns of afferent innervation of the core and shell in the "accumbens" part of the rat ventral striatum: immunohistochemical detection of retrogradely transported fluoro-gold. J. Comp. Neurol. *338*, 255–278.

Brown, T.E., Lee, B.R., Mu, P., Ferguson, D., Dietz, D., Ohnishi, Y.N., Lin, Y., Suska, A., Ishikawa, M., Huang, Y.H., et al. (2011). A silent synapse-based mechanism for cocaine-induced locomotor sensitization. J. Neurosci. *31*, 8163–8174.

Casassus, G., Blanchet, C., and Mulle, C. (2005). Short-term regulation of information processing at the corticoaccumbens synapse. J. Neurosci. *25*, 11504–11512.

Chao, J., and Nestler, E.J. (2004). Molecular neurobiology of drug addiction. Annu. Rev. Med. *55*, 113–132.

Conrad, K.L., Tseng, K.Y., Uejima, J.L., Reimers, J.M., Heng, L.J., Shaham, Y., Marinelli, M., and Wolf, M.E. (2008). Formation of accumbens GluR2-lacking AMPA receptors mediates incubation of cocaine craving. Nature *454*, 118–121.

Dong, Y., and Nestler, E.J. (2014). The neural rejuvenation hypothesis of cocaine addiction. Trends Pharmacol. Sci. *35*, 374–383.

Ferrario, C.R., Loweth, J.A., Milovanovic, M., Ford, K.A., Galiñanes, G.L., Heng, L.J., Tseng, K.Y., and Wolf, M.E. (2011). Alterations in AMPA receptor subunits and TARPs in the rat nucleus accumbens related to the formation of Ca^{2+}-permeable AMPA receptors during the incubation of cocaine craving. Neuropharmacology *61*, 1141–1151.

Grimm, J.W., Hope, B.T., Wise, R.A., and Shaham, Y. (2001). Neuroadaptation. Incubation of cocaine craving after withdrawal. Nature *412*, 141–142.

Groc, L., Gustafsson, B., and Hanse, E. (2006). AMPA signalling in nascent glutamatergic synapses: there and not there! Trends Neurosci. *29*, 132–139.

Hanse, E., Seth, H., and Riebe, I. (2013). AMPA-silent synapses in brain development and pathology. Nat. Rev. Neurosci. *14*, 839–850.

Huang, Y.H., Lin, Y., Mu, P., Lee, B.R., Brown, T.E., Wayman, G., Marie, H., Liu, W., Yan, Z., Sorg, B.A., et al. (2009). In vivo cocaine experience generates silent synapses. Neuron *63*, 40–47.

Huang, Y.H., Schlüter, O.M., and Dong, Y. (2013). An unusual suspect in cocaine addiction. Neuron *80*, 835–836.

Isaac, J.T., Nicoll, R.A., and Malenka, R.C. (1995). Evidence for silent synapses: implications for the expression of LTP. Neuron *15*, 427–434.

Jackson, M.E., and Moghaddam, B. (2001). Amygdala regulation of nucleus accumbens dopamine output is governed by the prefrontal cortex. J. Neurosci. *21*, 676–681.

Kalivas, P.W. (2004). Glutamate systems in cocaine addiction. Curr. Opin. Pharmacol. *4*, 23–29.

Kalivas, P.W. (2009). The glutamate homeostasis hypothesis of addiction. Nat. Rev. Neurosci. *10*, 561–572.

Kalivas, P.W., and McFarland, K. (2003). Brain circuitry and the reinstatement of cocaine-seeking behavior. Psychopharmacology (Berl.) *168*, 44–56.

Kasanetz, F., Deroche-Gamonet, V., Berson, N., Balado, E., Lafourcade, M., Manzoni, O., and Piazza, P.V. (2010). Transition to addiction is associated with a persistent impairment in synaptic plasticity. Science *328*, 1709–1712.

Kerchner, G.A., and Nicoll, R.A. (2008). Silent synapses and the emergence of a postsynaptic mechanism for LTP. Nat. Rev. Neurosci. *9*, 813–825.

Koya, E., Uejima, J.L., Wihbey, K.A., Bossert, J.M., Hope, B.T., and Shaham, Y. (2009). Role of ventral medial prefrontal cortex in incubation of cocaine craving. Neuropharmacology *56* (*Suppl 1*), 177–185.

Koya, E., Cruz, F.C., Ator, R., Golden, S.A., Hoffman, A.F., Lupica, C.R., and Hope, B.T. (2012). Silent synapses in selectively activated nucleus accumbens neurons following cocaine sensitization. Nat. Neurosci. *15*, 1556–1562.

Krettek, J.E., and Price, J.L. (1977). The cortical projections of the mediodorsal nucleus and adjacent thalamic nuclei in the rat. J. Comp. Neurol. *171*, 157–191.

LaLumiere, R.T., Smith, K.C., and Kalivas, P.W. (2012). Neural circuit competition in cocaine-seeking: roles of the infralimbic cortex and nucleus accumbens shell. Eur. J. Neurosci. *35*, 614–622.

Lee, B.R., and Dong, Y. (2011). Cocaine-induced metaplasticity in the nucleus accumbens: silent synapseH and beyond. Neuropharmacology *61*, 1060–1069.

Lee, B.R., Ma, Y.Y., Huang, Y.H., Wang, X., Otaka, M., Ishikawa, M., Neumann, P.A., Graziane, N.M., Brown, T.E., Suska, A., et al. (2013). Maturation of silent

synapses in amygdala-accumbens projection contributes to incubation of cocaine craving. Nat. Neurosci. *16*, 1644–1651.

Liao, D., Hessler, N.A., and Malinow, R. (1995). Activation of postsynaptically silent synapses during pairing-induced LTP in CA1 region of hippocampal slice. Nature *375*, 400–404.

Loweth, J.A., Scheyer, A.F., Milovanovic, M., LaCrosse, A.L., Flores-Barrera, E., Werner, C.T., Li, X., Ford, K.A., Le, T., Olive, M.F., et al. (2014). Synaptic depression via mGluR1 positive allosteric modulation suppresses cue-induced cocaine craving. Nat. Neurosci. *17*, 73–80.

MacAskill, A.F., Little, J.P., Cassel, J.M., and Carter, A.G. (2012). Subcellular connectivity underlies pathway-specific signaling in the nucleus accumbens. Nat. Neurosci. *15*, 1624–1626.

Malenka, R.C., and Bear, M.F. (2004). LTP and LTD: an embarrassment of riches. Neuron *44*, 5–21.

McCutcheon, J.E., Wang, X., Tseng, K.Y., Wolf, M.E., and Marinelli, M. (2011). Calcium-permeable AMPA receptors are present in nucleus accumbens synapses after prolonged withdrawal from cocaine self-administration but not experimenter-administered cocaine. J. Neurosci. *31*, 5737–5743.

McFarland, K., Lapish, C.C., and Kalivas, P.W. (2003). Prefrontal glutamate release into the core of the nucleus accumbens mediates cocaine-induced reinstatement of drug-seeking behavior. J. Neurosci. *23*, 3531–3537.

McGinty, V.B., and Grace, A.A. (2008). Selective activation of medial prefrontal-to-accumbens projection neurons by amygdala stimulation and Pavlovian conditioned stimuli. Cereb. Cortex *18*, 1961–1972.

Mogenson, G.J., and Yang, C.R. (1991). The contribution of basal forebrain to limbic-motor integration and the mediation of motivation to action. Adv. Exp. Med. Biol. *295*, 267–290.

Neisewander, J.L., Baker, D.A., Fuchs, R.A., Tran-Nguyen, L.T., Palmer, A., and Marshall, J.F. (2000). Fos protein expression and cocaine-seeking behavior in rats after exposure to a cocaine self-administration environment. J. Neurosci. *20*, 798–805.

Ozawa, S., Iino, M., and Tsuzuki, K. (1991). Two types of kainate response in cultured rat hippocampal neurons. J. Neurophysiol. *66*, 2–11.

Pascoli, V., Terrier, J., Espallergues, J., Valjent, E., O'Connor, E.C., and Lüscher, C. (2014). Contrasting forms of cocaine-evoked plasticity control components of relapse. Nature *509*, 459–464.

Peters, J., LaLumiere, R.T., and Kalivas, P.W. (2008). Infralimbic prefrontal cortex is responsible for inhibiting cocaine seeking in extinguished rats. J. Neurosci. *28*, 6046–6053.

Pickens, C.L., Airavaara, M., Theberge, F.R., Fanous, S., Hope, B.T., and Shaham, Y. (2011). Neurobiology of the incubation of drug craving. Trends Neurosci. *34*, 411–420.

Reep, R. (1984). Relationship between prefrontal and limbic cortex: a comparative anatomical review. Brain Behav. Evol. *25*, 5–80.

Robinson, T.E., Gorny, G., Mitton, E., and Kolb, B. (2001). Cocaine self-administration alters the morphology of dendrites and dendritic spines in the nucleus accumbens and neocortex. Synapse *39*, 257–266.

Scheuss, V., and Neher, E. (2001). Estimating synaptic parameters from mean, variance, and covariance in trains of synaptic responses. Biophys. J. *81*, 1970–1989.

Schmidt, H.D., Anderson, S.M., Famous, K.R., Kumaresan, V., and Pierce, R.C. (2005). Anatomy and pharmacology of cocaine priming-induced reinstatement of drug seeking. Eur. J. Pharmacol. *526*, 65–76.

See, R.E. (2005). Neural substrates of cocaine-cue associations that trigger relapse. Eur. J. Pharmacol. *526*, 140–146.

Sesack, S.R., Deutch, A.Y., Roth, R.H., and Bunney, B.S. (1989). Topographical organization of the efferent projections of the medial prefrontal cortex in the rat: an anterograde tract-tracing study with Phaseolus vulgaris leucoagglutinin. J. Comp. Neurol. *290*, 213–242.

Silver, R.A. (2003). Estimation of nonuniform quantal parameters with multiple-probability fluctuation analysis: theory, application and limitations. J. Neurosci. Methods *130*, 127–141.

Stefanik, M.T., Moussawi, K., Kupchik, Y.M., Smith, K.C., Miller, R.L., Huff, M.L., Deisseroth, K., Kalivas, P.W., and LaLumiere, R.T. (2013). Optogenetic inhibition of cocaine seeking in rats. Addict. Biol. *18*, 50–53.

Suska, A., Lee, B.R., Huang, Y.H., Dong, Y., and Schlüter, O.M. (2013). Selective presynaptic enhancement of the prefrontal cortex to nucleus accumbens pathway by cocaine. Proc. Natl. Acad. Sci. USA *110*, 713–718.

Sutton, M.A., Schmidt, E.F., Choi, K.H., Schad, C.A., Whisler, K., Simmons, D., Karanian, D.A., Monteggia, L.M., Neve, R.L., and Self, D.W. (2003). Extinction-induced upregulation in AMPA receptors reduces cocaine-seeking behaviour. Nature *421*, 70–75.

Wolf, M.E., and Ferrario, C.R. (2010). AMPA receptor plasticity in the nucleus accumbens after repeated exposure to cocaine. Neurosci. Biobehav. Rev. *35*, 185–211.

Wolf, M.E., and Tseng, K.Y. (2012). Calcium-permeable AMPA receptors in the VTA and nucleus accumbens after cocaine exposure: when, how, and why? Front. Mol. Neurosci. *5*, 72.